

# ArtisanGS: Interactive Tools for Gaussian Splat Selection with AI and Human in the Loop

CLEMENT FUJI TSANG, NVIDIA, Canada

ANITA HU, NVIDIA, Canada

OR PEREL, NVIDIA and University of Toronto, Canada

CARSTEN KOLVE, NVIDIA, France

MARIA SHUGRINA, NVIDIA and University of Toronto, Canada



Fig. 1. **From messy kitchens to interactive objects:** Our goal is to enable 3D practitioners to source objects from in-the-wild captures and work with them for emerging downstream applications, such as editing and physics simulation. To touch the tip of the iceberg on this topic, we propose a suite of interactive techniques for selection of objects and parts in 3D Gaussian Splat scenes, enabling applications like targeted editing.

Representation in the family of 3D Gaussian Splats (3DGS) are growing into a viable alternative to traditional graphics for an expanding number of application, including recent techniques that facilitate physics simulation and animation. However, extracting usable objects from in-the-wild captures remains challenging and controllable editing techniques for this representation are limited. Unlike the bulk of emerging techniques, focused on automatic solutions or high-level editing, we introduce an interactive suite of tools centered around versatile Gaussian Splat selection and segmentation. We propose a fast AI-driven method to propagate user-guided 2D selection masks to 3DGS selections. This technique allows for user intervention in the case of errors and is further coupled with flexible manual selection and segmentation tools. These allow a user to achieve virtually any binary segmentation of an unstructured 3DGS scene. We evaluate our toolset against the state-of-the-art for Gaussian Splat selection and demonstrate their utility for downstream applications by developing a user-guided local editing approach, leveraging a custom Video Diffusion Model. With flexible selection tools, users have direct control over the areas that the AI can modify. Our selection and editing tools can be used for any in-the-wild capture without additional optimization.

Authors' Contact Information: Clement Fuji Tsang, [caenorst@hotmail.com](mailto:caenorst@hotmail.com), NVIDIA, Canada; Anita Hu, [anitah@nvidia.com](mailto:anitah@nvidia.com), NVIDIA, Canada; Or Perel, [orr.perel@gmail.com](mailto:orr.perel@gmail.com), NVIDIA and University of Toronto, Canada; Carsten Kolve, [carsten.kolve@gmail.com](mailto:carsten.kolve@gmail.com), NVIDIA, France; Maria Shugrina, [shumash@gmail.com](mailto:shumash@gmail.com), NVIDIA and University of Toronto, Canada.

## 1 Introduction

Recent methods for multi-view capture, such as 3D Gaussian Splats (3DGS) [Kerbl et al. 2023], have reduced the barrier around capturing high-fidelity realistic 3D scenes. With other advances, such as representation-agnostic physics simulation [Modi et al. 2024] and generative capabilities [Yi et al. 2024], 3DGS representation and its variants [Huang et al. 2024; Moenne-Loccoz et al. 2024] are on track to become a feasible alternative to mesh-based graphics for many interactive applications. For example, interactive 3D scenes could be authored from videos captured in the wild; realistic simulation environments for robotics could be created by simply recording the real world. However, a tangible lack of tools for processing 3DGS captures into interactive scenes, including fine segmentation and targeted editing tools, hinders these applications in practice.

We propose ArtisanGS, a suite of AI-powered and user-driven tools for flexible selection of 3DGS objects from unstructured in-the-wild captures (§4). Our selection tools are designed to work in conjunction with other applications (§6) needing local control like 'editing'. We enable workflows where 3DGS objects are separated from the rest of the scan, processed and then re-composed into the original 3d capture or novel environment - which in turn enables interactive applications for games and robotics.

Working with monolithic 3DGS captures is challenging due to their unstructured nature. To enable object-based interactions, Gaussians representing specific objects must be **segmented**. While several prior works address AI-based semantic grouping and masking of Gaussians (Tb.1), most require lengthy training and none offer strategies to correct mistakes, which makes these methods difficult to apply in practice. In contrast, emerging commercial tools (see Supplemental) primarily target laborious manual operations. We design versatile interactive tool that allows a user to work with minimal-input AI-assisted 3D segmentation (often just one or two clicks), diagnose and correct mistakes, and manually target specific areas. We develop a clean and consistent treatment of 2D and 3D selections in our toolkit design, enabling users to jump between different selection modes. Together, these techniques enable 3D artists to achieve nearly any desired 3D segmentation fast.

Flexible 3D selection empowers many applications (§6) that benefit from targeted control. As one example, we develop local editing of segmented 3DGS objects guided by user selections with a custom object-centric Video Diffusion Model. We also show how selection tools can facilitate guided scene orientation and enable scene setup and material assignment for applications like physics simulation, now possible directly over 3DGS objects [Modi et al. 2024].

In summary, our contributions are as follows:

- Interactive 3D segmentation method for 3DGS objects, powered by pre-trained 2D segmentation networks, requiring a single click or 2D mask for any one view (no offline scene-based optimization)
- Quantitative and qualitative evaluation of this selection against baselines and commercial software
- Technique to allow users to diagnose and correct errors in the above nearly automatic segmentation
- Interactive techniques allowing users to employ a 2D segmentation network or traditional 2D segmentation tools for manual clean-up of 3D segmentation
- Demonstration of possible applications that could be facilitated by flexible 3DGS selection

Our method can be applied to any messy in-the-wild-capture, without requiring original training views or scene-specific pre-training. We prototype an interface to show the utility of our selection and segmentation toolkit design.

## 2 Related Work

### 2.1 Multi-View 3D Capture

Many recent methods focused on optimizing a 3D representation of a scene based on multi-view photographs. Following a rich line of work based on Neural Radiance Fields (NERFs) [Mildenhall et al. 2021], a recently popular 3D representation for multi-view 3D captures is 3D Gaussian Splatting (3DGS) [Kerbl et al. 2023]. While, like NERF, vanilla 3DGS suffers from baked lighting, which becomes obvious during scene manipulation, many emerging works are extending this representation to be more in line with physics based rendering [Du et al. 2024; Gao et al. 2025; Liang et al. 2024; Moenne-Locozoz et al. 2024]. Unlike NERF, its many variants [Müller et al. 2022; Wang et al. 2023], and grid-based alternatives such as [Fridovich-Keil et al. 2022], which are difficult to manipulate locally,

the explicit nature of 3DGS makes this representation family [Huang et al. 2024; Kerbl et al. 2023; Moenne-Locozoz et al. 2024; Rong et al. 2024] convenient for editing and local transformations. This has led to an exciting line of work that uses 3DGS for physical interaction and direct manipulation [Jiang et al. 2024; Modi et al. 2024; Xie et al. 2023; Zhao et al. 2024], or allows sophisticated editing [Chen et al. 2024a; Liu et al. 2024a]. However, a prerequisite for most applications of this kind is segmenting individual objects or parts from the 3DGS scene, where existing methods fall short in flexibility.

### 2.2 Segmenting 3D Gaussian Splats

A wide range of works address segmentation of 3DGS scenes, with the most notable tabulated in Tb.1. Many prior methods devise per-scene learning techniques (Tb.1, per-scene training) to counter mask inconsistencies of 2D segmentation networks like SAM [Kirillov et al. 2023], resulting in per-Gaussian feature vectors. Feature3DGS [Zhou et al. 2024] distill general 2D features, not focusing specifically on segmentation, while other approaches of this class typically use SAM or another 2D segmentation network. GaussianGrouping [Ye et al. 2025] propagates IDs using off-the-shelf tracker [Cheng et al. 2023], and imposes regularization losses. ClickGaussian [Choi et al. 2025], GARField [Kim et al. 2024], SAGA [Cen et al. 2023], SegWild [Bao et al. 2025] and OmniSeg3D [Ying et al. 2024] all perform scale-aware or hierarchical contrastive learning to ensure multi-view feature consistency, while EgoLifter’s [Gu et al. 2025] contrastive learning takes special care of dynamic objects. These approaches are effective at generating a pre-processed version of the scene that could be used for semantic reasoning and once trained allow segmenting out 3D Gaussians based on queries such as feature proximity to one or several points. Beyond the time-consuming scene pre-processing, which takes tens of minutes to hours, depending on the method, this class of techniques is inherently limited in their flexibility. While these approaches implement slightly different interfaces and strategies for converting features to 3D masks,

Method	Features training	Seg. time
ClickGaussian [Choi et al. 2025]	yes	10 ms
OmniSeg3D [Ying et al. 2024]	yes	not reported
GARField [Kim et al. 2024]	yes (bndl)	320ms / lvl
Gau-Grouping [Ye et al. 2025]	yes (bndl)	1.2s
EgoLifter [Gu et al. 2025]	yes (bndl)	not reported
Feature3DGS [Zhou et al. 2024]	yes	not reported
FlashSplat [Shen et al. 2025]	no	30s
GaussianEditor [Chen et al. 2024a]	no	40s
iSegMan [Zhao et al. 2025]	yes	4-6s
Seg-Wild [Bao et al. 2025]	yes	not reported
<b>pre-prints</b>		
SAGA [Cen et al. 2023]	yes	4ms
CoSeg [Dou et al. 2024]	yes	not reported
GaussianCut [Jain et al. 2024]	no	50-120s
<b>Ours</b>	no	1-5s

Table 1. 3D Segmentation methods for 3D Gaussian Splats, prioritizing methods that take some form of user input. Many approaches require Features training or extraction for every input scene, where in some cases this step is bundled into original 3DGS training (noted as "(bndl)"). When reported, segmentation time is listed, given user input such as a target click.

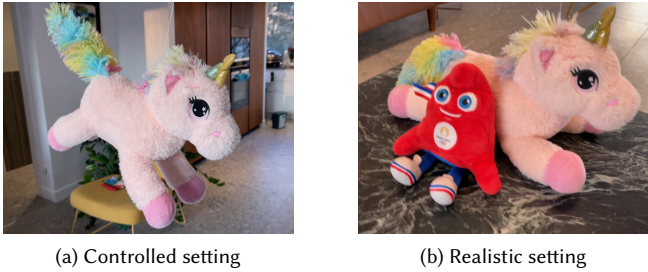


Fig. 2. **3D Capture Setups:** While segmenting objects from controlled captures, like the toy suspended by wires (a), is relatively simple with existing tools, these solutions fall short on more realistic use cases (b).

mistakes, noise and biases are inevitably pre-baked into the feature field. It is impossible for the user to deviate from the types of masks used for pre-training or to correct mistakes beyond adding additional target feature vectors. Many of the same limitations apply to RT-GS2 [Jurca et al. 2024], the only generalizable technique involving semantic feature learning, which trains a set of networks on a small dataset of scenes, but it is not clear if this work can generalize beyond indoor environments, and only 2D novel view segmentation results are presented.

The approaches that generate 3D segmentation without special pre-training are more similar to our method. Like ours, most begin with a user-provided 2D mask, typically generated with a pre-trained network like SAM. Several methods require initial user clicks, project these clicks onto 3D Gaussians and track these 3D points [Chen et al. 2024a; Hu et al. 2024a; Shen et al. 2025] or epipolar line [Zhao et al. 2025] to generate SAM queries for other views, an approach that can break down for far away views and is too tied to click-based input, making it impossible to e.g. manually annotate a mask. GaussianCut [Jain et al. 2024] is the only one leveraging a video mask tracking network to propagate a single 2D mask to other views, but it likewise does not offer strategies to correct mistakes. We instead choose to use Cutie [Cheng et al. 2024] for mask tracking, which due to the unique design of its memory frames, makes our interactive segmentation amenable to user correction. Once a 2D mask is extended to multi-view masks, these are aggregated to 3D Gaussian labels. GaussianEditor [Chen et al. 2024a], SAGD [Hu et al. 2024a] (previously SAGS [Hu et al. 2024b]), iSegMan [Zhao et al. 2025] and [Joseph et al. 2024] devise voting schemes for assigning per-Gaussian labels, while FlashSplat formulates the segmentation as an integer linear programming optimization [Shen et al. 2025] and GaussianCut [Jain et al. 2024] a graph cut problem. Our solution is faster than most others (See Tb.1) and easier to extend to alternative 3DGS formulations, because we treat differentiable splat renderer as a black box component. Given limited available benchmarks, our approach offers comparative quality to other others and, unlike prior methods, allows users many strategies to correct mistakes in the initial segmentation. In addition, we discuss emerging software tools in the Supplemental Material and our video.

### 2.3 Editing Applications on Splats

Several approaches touch on interactive, prompt-based or style-driven editing of 3DGS scenes [Chen et al. 2024a; Jiang et al. 2024;

Liu et al. 2024b; Palandra et al. 2024; Vachha and Haque 2024; Wu et al. 2025; Yi et al. 2024], but in most cases allowing users targeted control over the modified area is at best an afterthought. We show that the flexible selection and segmentation tools in ArtisanGS can enable more controllable editing applications for 3DGS. Similarly, works targeting inpainting of 3D captured scenes [Barda et al. 2024; Chen et al. 2024b; Lu et al. 2024; Weber et al. 2024] focus on removing or hallucinating entire objects, typically assuming that the mask or target area is given. Lack of appropriate tools makes these techniques difficult to test on in-the-wild scenes, where targeted masks are difficult to obtain. Our goal is to enable this line of research to address more targeted editing and completion of 3DGS scenes, to enable crafting interactive applications from in-the-wild captures. As an illustration, we develop a prototype editing application by building on work in controllable video diffusion models [Hong et al. 2022; Xu et al. 2024; Yang et al. 2024].

## 3 Preliminaries

### 3.1 Motivation

Multi-view captures like NERFs and 3D Gaussian Splats (3DGS) have fascinated practitioners with their ability to effortlessly reconstruct highly realistic 3D environments. However, for practical applications, these environments remained largely static, confined to novel view synthesis. Recent advances offering practical solutions for dynamic effects on 3DGS scenes, including physics simulation [Modi et al. 2024; Xie et al. 2023] and relighting [Gao et al. 2025], are promising to bring 3DGS into dynamic applications. While individual high-quality 3DGS objects can be reconstructed from highly controlled capture setups (e.g. suspended by wires in Fig.2a), this severely limits ability to capture more realistic scenes (Fig.2b) or work with videos and splat models available online. Extracting usable objects from such in-the-wild 3DGS scenes is prohibitively difficult with the current state of tools, a gap that we address in this work.

### 3.2 Method Overview

Imagine working with a monolithic capture of a cluttered environment, like a play room. To construct an interactive environment, this scene must first be broken apart into individual objects. This is the core task addressed by our method in §4, showing why fully automatic solutions do not work perfectly, and how the user could more directly control the final output. Flexible selection forms the necessary backbone for many applications.

Once segmented, the object or a scene might have arbitrary orientation, making everything, starting with camera control, more challenging. Occlusions within the scene will also inevitably cause parts of the captured objects to be missing. Unless perfectly choreographed, source views will also contain varying level of detail for different view angles, resulting in areas of degraded quality around the object, which may need local targeted editing and refinement. In §6, we show how our selection and segmentation tools can feed into such applications for 3DGS object processing, including orientation §6.1 and an early prototype of local editing §6.2.

The clean and consistent design of 2D and 3D selection in our toolkit combines automatic AI-driven techniques with user input and could be integrated into future end-user applications for crafting

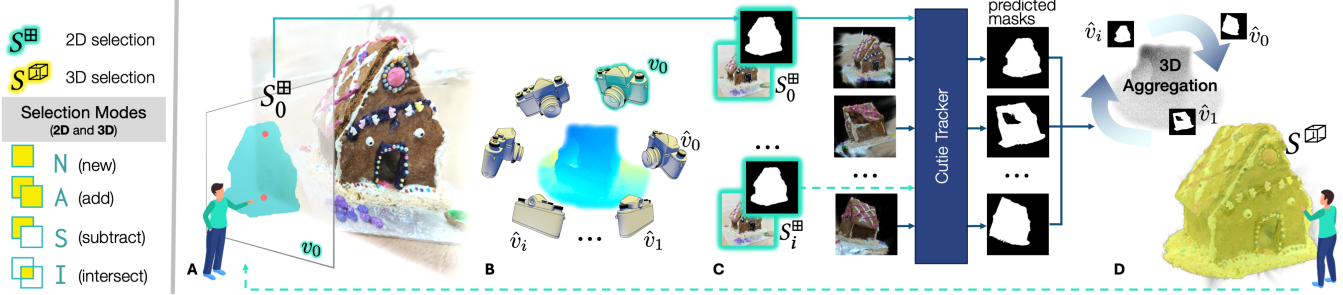


Fig. 3. **Auto-Tracked Segmentation with Corrections**: We propose automatic way to project 2D user masks  $S_i^{\boxplus}$  to 3D selection  $S^{\boxplus}$  over 3D Gaussians, while allowing users to correct the outcome (§4.4). **Left**: notation and selection modes supported in our design (§4).

interactive 3DGS scenes. As a sample application, we show physics simulation with Simplicits [Modi et al. 2024] on scenes processed with our technique (§6.3).

### 3.3 Definitions

We start with a pre-trained 3DGS scene [Kerbl et al. 2023], containing a set  $\mathcal{G}$  of  $n$  individual 3D Gaussians  $G_i$ , each with a position  $\mu_i$ , covariance  $\Sigma_i$ , view-dependent color and opacity  $\alpha_i$ . We assume the existence of optimized differentiable rendering kernels for  $\mathcal{G}$ , including  $\text{render}(\mathcal{G}, v)$  producing RGBA rendering of the 3DGS scene from camera view  $v$ ,  $\text{depth}(\mathcal{G}, v)$  producing camera-space depth rendered from  $v$ ,  $\text{features}(\mathcal{G}, v, F)$  rendering any custom per-Gaussian feature vectors  $F := \{F_0 \dots F_n\}$ , *viz*  $(\mathcal{G}, v)$  producing a binary mask specifying the Gaussians visible from  $v$  and  $\text{first\_hits}(\mathcal{G}, v)$  outputting the id of the first hit Gaussian per pixel. Our method does not assume anything beyond the existence of these functions and so is in principle applicable to alternative 3DGS variants such as [Huang et al. 2024; Moenne-Loccoz et al. 2024], but we have run all our experiments on the original formulation [Kerbl et al. 2023], trivial to extend to  $\text{depth}(\mathcal{G}, v)$  and  $\text{features}(\mathcal{G}, v, F)$  by applying the original  $\text{render}(\mathcal{G}, v)$  function to other per-Gaussian features.

Typically,  $\mathcal{G}$  has high-quality appearance from camera views that do not stray too far from the training views  $\bar{V} := \{\bar{v}_0 \dots \bar{v}_n\}$  used for optimization, but may appear foggy or abstract from views that are not well-represented (Fig.1), which can affect the result of AI models trained on real images. While we do not assume the knowledge of  $\bar{V}$ , our algorithm has the option of using them if available.

## 4 Interactive Segmentation

We will now present an interactive toolkit for 3DGS selection and segmentation. We define the segmentation problem as selecting a subset of Gaussians  $\mathcal{S} \in \mathcal{G}$  according to the user intent. Any implementation of our proposed toolkit will allow users control of the camera view  $v_c$  and will keep track of the 2D segmentation mask  $S^{\boxplus}$  (active for  $v_c$ ) and of the current 3D segmentation mask  $S^{\boxplus}$ , containing a binary value for every element of  $\mathcal{G}$ . We will use  $\mathcal{S}$  to refer to the subset of Gaussians currently in  $S^{\boxplus}$ . Different color is used to denote 2D and 3D selections in our diagrams and in our UI to make them easier to distinguish (See Fig.3).

Given preliminary requirements (§4.1, §4.2), we propose combining multiple ways to project 2D masks to  $S^{\boxplus}$ . First, we show simple

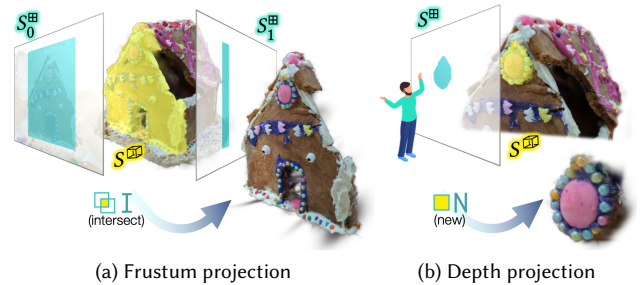


Fig. 4. **Manual Projection** (§4.3) of 2D masks  $S_i^{\boxplus}$  to 3D, combined with different selection modes (§4.1), allow flexible manual selection.

yet powerful manual projection modes (§4.3), and then detail our automatic mask tracking and segmentation method in §4.4.

### 4.1 Selection Modes

Established image selection tools in software like Photoshop support the following major modes: new (N) - replace current selection, add to (A), subtract from (S) and intersect with (I) the current selection. To provide consistent experience, we support all of these modes both for 2D selection and 3D selection (Fig.3, left). In both cases, the modes correspond to boolean operations on the active image mask  $S^{\boxplus}$  or binary per-Gaussian mask  $S^{\boxplus}$ . In our implementation, N is the default mode, and others are activated through Ctrl, Alt and Shift modifiers, but many other UI designs are possible.

### 4.2 Required 2D Mask Capabilities

Because users can only see a 2D rendering of  $G$ , 2D selection is a necessary prerequisite for any 3D selection interface. While any 2D image segmentation techniques could be used in combination with our toolkit, it is critical to allow users a variety of 2D masking tools to bootstrap interactive 3D segmentation below. Our particular implementation, like others before it, allows users to generate a mask  $S^{\boxplus}$  for any view  $v_c$  from one or more positive and negative clicks using SAM [Kirillov et al. 2023], but other models could be used instead. We also allow manually painting 2D areas and drawing 2D bounding boxes, while supporting the selection modes in §4.1.

### 4.3 Manual 2D to 3D Projection Modes

In addition to automatic aggregation (§4.4 to follow), our design supports two manual modes of projecting user’s 2D selection to 3D. The *frustum projection* mode selects all Gaussians, for which the mean projects into the current mask  $S_c^{\boxplus}$  of the current view  $v_c$ . This effectively selects all the Gaussians falling into the sweep of  $S_c^{\boxplus}$  through the camera frustum. Coupled with the selection modes in §4.1, frustum projection is surprisingly effective for some use cases. In Fig.4a, projection of  $S_0^{\boxplus}$  followed by projection of  $S_1^{\boxplus}$  with mode  $\text{I}$  (intersect), effectively selects the facade of the gingerbread house.

In some cases, selecting surface layer is more desirable. In the *depth projection* mode, we select all the Gaussians that are in the frustum projection of  $S^{\boxplus}$  and also lie within a threshold of the rendered depth at their location. This mode allows picking up surface detail, such as the wreath in Fig.4b.

### 4.4 Auto-Tracked Segmentation with Corrections

We propose a fast automatic way to convert one or more user-provided 2D masks  $S_0^{\boxplus} \dots S_k^{\boxplus}$  corresponding to views  $v_0 \dots v_k$  to a 3D Gaussian mask  $S^{\boxplus}$  (Fig.3). Like other training-free approaches for this task [Chen et al. 2024a; Hu et al. 2024a; Jain et al. 2024; Shen et al. 2025], we generate multi-view masks (§4.4.2) for a dense set of views (§4.4.1) and then aggregate these masks into a 3D mask (§4.4.3). Uniquely, our approach allows users visibility into the method and ability to correct mistakes (§4.4.4).

**4.4.1 Selecting Dense Views.** We support multiple ways to sample dense views around the target object. If the training views  $\bar{V}$  are available, all or a subset can be used. Training views are guaranteed to show the scene from a well-optimized angle, but may be very zoomed out for large scenes. In addition, requiring training views would also constrain the types of captures that could be segmented. Therefore, we devise an alternative method, using the point cloud obtained by lifting  $\text{first\_hits}(\mathcal{G}, v_0)$  from the masked area  $S_0^{\boxplus}$ . We turn the camera around the center of this point cloud, doing a full circle trajectory on the plane defined by the camera up axis, and use the corresponding user view  $v_0$  for up direction and distance from the look at point. We ablate the choice of training or camera turnaround views in our results section. Note that the number of views used for tracking ( $m$ ), is an important hyperparameter for our method’s speed, but we found it to work robustly when sampling about 50 views (See §5.3).

**4.4.2 Obtaining Multi-View Masks.** Similarly to ours, many training-free prior methods tackling 3DGS segmentation start with a mask  $S_0^{\boxplus}$  and then use it to obtain  $m$  multi-view masks  $S_0^{\boxminus} \dots S_m^{\boxminus}$  for the dense views  $\hat{v}_0 \dots \hat{v}_m$ . Most of these techniques [Chen et al. 2024a; Hu et al. 2024a; Shen et al. 2025] track depth-projected query points from the first mask to generate SAM queries for other views. This approach can cause errors for more extreme views where 3D query points are not visible and leaves the result at the mercy of a specific click-based network like SAM [Kirillov et al. 2023]. In contrast, we rely on a robust mask tracking network Cutie [Cheng et al. 2024]. This design decision results in more robust tracking, and supports our goal of allowing users to add more guidance when needed.

The network architecture and inference pipeline of Cutie accepts object-level conditioning through one or more reference frames, injected at appropriate points in the video sequence due to memory constraints (See user masks  $S_i^{\boxplus}$  in Fig.3C). To facilitate attending to appropriate annotations, we shift the target turnaround views  $\hat{v}_0 \dots \hat{v}_m$  to begin with the optimal view angle, obtaining shifted sequence  $\hat{v}_0 \dots \hat{v}_m$  (Fig.3B). We select the first view  $\hat{v}_0$  to be  $\hat{V}^*(v_0)$ , defined as the target view  $\hat{v}_i$  that is most similar to the annotated view  $v_0$  according to the following criterion:

$$\hat{V}^*(v) := \operatorname{argmin}_{\hat{v}_j} J(\text{viz}(\mathcal{G}, v), \text{viz}(\mathcal{G}, \hat{v}_j)) \quad (1)$$

where  $\text{viz}$  is the visibility mask defined in §3.3, and  $J$  is the Jaccard index. Thus, Cutie is injected with the user mask  $S_0^{\boxplus}$  and corresponding  $\text{render}(\mathcal{G}, v_0)$  right before predicting the mask for the most similar view  $\hat{v}_0$ . Given multiple user masks  $S_i^{\boxplus}$  for the views  $v_i$ , each  $S_i^{\boxplus}$  and  $\text{render}(\mathcal{G}, v_i)$  is injected as a memory frame prior to predicting the corresponding most similar target view  $\hat{V}^*(v_i)$ . This approach allows users to annotate any number of frames for any view angle, without being constrained to pre-selected views.

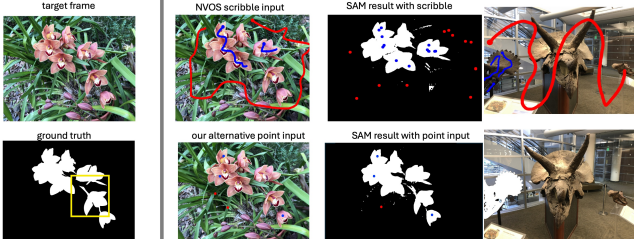
**4.4.3 Aggregating to 3D.** Given user masks  $S_0^{\boxplus} \dots S_k^{\boxplus}$  for views  $v_0 \dots v_k$ , and automatically tracked masks  $S_0^{\boxminus} \dots S_m^{\boxminus}$  for dense views  $\hat{v}_0 \dots \hat{v}_m$ , we now aggregate them into a binary mask  $S^{\boxplus}$  over the Gaussians (Fig.3D). Instead of devising a custom voting scheme like [Chen et al. 2024a; Hu et al. 2024a] specific to a particular 3DGS variant, or formulating a linear programming [Shen et al. 2025] or graph cut problem [Jain et al. 2024], which has additional complexity and overhead, we simply leverage the fast differentiable 3DGS renderer to optimize the mask assignment. Specifically, we run a single loop over the views  $\hat{v}_0 \dots \hat{v}_m, v_0 \dots v_k$ , optimizing a one channel feature  $M$  for each Gaussian with an L2 image loss between the 2D masks and  $\text{features}(\mathcal{G}, v, M)$ . We found it effective to simply set the binary  $S^{\boxplus}$  to  $M > 0.5$ , a setting we use for all demos and experiments. The “black-box” treatment of 3DGS renderer makes this aggregation applicable to other point splatting formulations like [Huang et al. 2024; Moenne-Loccoz et al. 2024].

**4.4.4 User Corrections.** Crucially, unlike prior methods, we also allow users to diagnose the cause of error in the 3d aggregation. Using our UI, users can browse automatic masks generated by Cutie and add more masks for any additional view via SAM annotation or manual mask painting. The annotated views are inserted into the Cutie inference based on their proximity with the target views for which automatic masks are being generated (§4.4.2), resulting in a more robust turnaround performance and better aggregation.

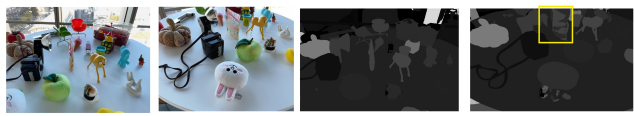
**4.4.5 Performance Improvements.** The performance of any method leveraging 2D masks for 3D aggregation is sensitive to occlusions around the object. To improve performance of our method in cluttered scenes, we give users the option to mark a mask as containing no occlusions. When such masks are provided (default setting), we first pre-segment the scene using intersecting frustum projections (§4.3) of these masks and perform tracking (§4.4.2) and aggregation (§4.4.3) only on this segment. This optimization not only improves robustness to occlusions, but also the speed of the aggregation due to faster rendering.

## 5 Results and Evaluation

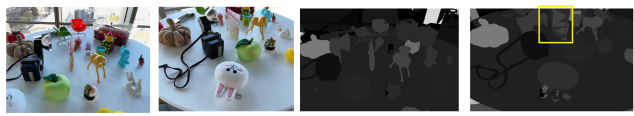
In this section, we evaluate our auto-tracked segmentation (§4.4) quantitatively (§5.1), show qualitative comparisons with related selection and segmentation tools (§5.2) and present ablations (§5.3). See the following section §6 for applications.



(a) NVOS scribbles vs. our alternative SAM queries.



(b) NVOS occl.



(c) Large inaccuracies in automatic masks of LERF-mask

Fig. 5. **Evaluation Datasets:** Annotations on both NVOS (a) and LERF-Mask (b) have inaccuracies. We suggest alternative inputs for NVOS (a)

### 5.1 Quantitative Evaluation

**5.1.1 Baselines.** We compare our segmentation against FlashSplat[Shen et al. 2025] and GaussianCut[Jain et al. 2024], which, similarly to our method, require no pre-processing of the input scene (See segmentation methods in Tb.1). In addition, we compare against SAGA[Cen et al. 2023], GaussianGrouping [Ye et al. 2025], iSegMan[Zhao et al. 2025] and OmniSeg3D[Ying et al. 2024], competitive methods that need scene pre-processing in order to allow segmentation. Note that our method was developed in 2024 and we may be missing some more recent techniques in this evaluation.

**5.1.2 Datasets and Metrics.** There is no robust and diverse benchmark for the segmentation task that we target. Commonly used NVOS [Ren et al. 2022] dataset is very small, and LERF-Mask [Ye et al. 2025] contains noisy auto-labels (e.g. see noisy auto-labels in Fig.5c). Because most baselines use this dataset, we report results on the smaller, more accurate NVOS dataset [Ren et al. 2022], consisting of a small number of front-facing scenes from LLFF [Mildenhall et al. 2019] with target scribbles in one frame and a single ground truth mask for another frame. The input scribbles in NVOS are an imperfect representation of user intent, and fail with modern segmentation methods that rely on clicks, such as SAM [Kirillov et al. 2023] (See Fig.5, where scribbles are not placed on all the target flowers, confusing SAM). While many of the baselines we compare with also rely on input clicks, the codebases and papers of FlashSplat[Shen et al. 2025], SAGA[Cen et al. 2023], GaussianCut[Jain et al. 2024] and OmniSeg3D[Ying et al. 2024] do not include the exact logic for sampling points from NVOS scribbles or the number of points. However, these details have a pronounced effect on click-based methods, like SAM, and make reported numbers from these related works that are using random sampling from the scribbles

Method	mIoU↑	Acc↑
FlashSplat	91.8	98.6
GaussianCut	92.5	98.4
Gaussian Grouping	90.6	98.2
SAGA	90.9	98.3
iSegMan	92.0	98.4
OmniSeg3D	91.7	98.4
OmniSeg3D (with our points)	78.5	96.4
Ours (with pre-segment)	82.4	98.1
Ours (without pre-segment)	<b>94.1</b>	<b>98.8</b>

Table 2. Segmentation Eval on NVOS.

unreliable.<sup>1</sup> Nonetheless, we include a comparison for completeness, and report click sampling logic here. Because our method starts with a user-annotated mask, failing due to bad SAM initialization would not meaningfully evaluate our method. Instead of NVOS scribbles, we provide a small number (1 to 6) of positive point inputs for the starting frame, and use the same ground truth frame to evaluate. For all baselines, we report original NVOS results, with point click logic tuned for their method, and for OmniSeg3D [Ying et al. 2024], the best available method with a released codebase, we additionally show performance on our input point clicks. We use standard metrics of pixel classification accuracy (Acc) and foreground intersection-over-union (IoU). At best, NVOS provides a very noisy estimate of performance due to its tiny size and carefully choreographed front-facing scenes, but we include it as the standard benchmark reported in literature, and later focus on qualitative differences that make our method easy to apply in practice (§5.2).

**5.1.3 Results.** Results in Tb.2, showing competitive performance of our method against baselines, while also being faster, and requiring no scene pre-processing (See Tb.1 for prior method properties and speed). Because point sampling results in noisy results (see above), we did not reevaluate the baselines under the slightly different setting of click inputs rather than scribbles. However, for the competitive OmniSeg3D, our point samples result in severely degraded performance, suggesting that their technique requires a lot more points to work accurately, and suggesting that custom point sampling logic of prior works is likely designed to their advantage. In all cases, our technique outperforms others when pre-segmentation (§4.4.5 is turned off, and degraded performance is due to a single example ("horns left") where the annotated frame does not include the whole target object (Fig.5b). In practice, when using our method, users have a choice to enable the pre-segmentation optimization. We next provide qualitative evaluation, showing that our technique may be easier to apply in practice, allowing user-driven segmentation with corrections.

### 5.2 Qualitative Results

Qualitatively, we compare our method against one pre-training method [Kim et al. 2024] and the training-free GaussianEditor [Chen et al. 2024a] approach. We use in-the-wild captured scenes or challenging 360-degree scenes from LERF [Kerr et al. 2023] that are

<sup>1</sup>To quantify the effect of point sampling, we ran SAM segmentation on one of the NVOS images 20 times, using randomized 3 to 10 positive and 1 to 4 negative clicks. The resulting masks have an average pairwise IoU of 68.3%, and it can be as small as 3.5% between runs, showing the overwhelming effect of point choices on performance.

closer to our target use case. While in the paper, GaussianEditor reports better performance, we found its segmentation running in around 40s on a higher-end GPU, making any sort of interaction or iteration difficult. Unlike GaussianEditor in practice, our method runs in 1-5 seconds on the same hardware, enabling interactive iteration over the target segmentation and user inputs. Critically, we also allow users to correct both automatic masks or perform segmentation manually (§4.3). We also observe more frequent mistakes for similar examples in Fig.8d. As described in the related work, Garfield [Kim et al. 2024] suffers from features that are pre-baked during training and can make finer-grained segmentation difficult. On the LERF figurines scene, Garfield shows similar performance on simple objects, but for more complex examples like "Charlie" in the Twizzlers box or the camera with the strap, Garfield's discrete Group Level parameter is insufficient to select the target object and its thin parts (Fig.8f), while our automatic tracking with a single reference easily selects these. We also made an effort to run FlashSplat [Shen et al. 2025], but ran into technical issues not addressed by the authors (URL). Comparing to manual segmentation with software tool SuperSplat [PlayCanvas 2024] (Fig.8e), we found SuperSplat very difficult and time-consuming to use, especially when separating objects from surfaces and dealing with stacked objects. On the other hand, our method is a lot faster and user-friendly, providing a good initial segmentation using SAM selection, and allowing additional manual fine-tuning only if necessary. We believe that it strikes just the right balance between automation and user intervention, allowing selecting virtually any desirable subset of Gaussians given user intent. See §6 for possible applications of such segmentation, and Supplemental Video (soon to be uploaded) for additional qualitative results.

### 5.3 Ablations

For ablations, we used LERF [Kerr et al. 2023] figurines scene, a challenging 360-degree scene. Because the automatic mask annotations in LERF-Mask [Ye et al. 2025] are very noisy (Fig.5c), we instead hand annotated the pretrained 3DGS scene without using any automatic segmentation, using only manual 2D bounding box selections with the frustum projection described in (§4.3). For each object, we additionally annotate input SAM queries and the corresponding mask for one training view (input view: train) and for one additional view outside of the training view trajectory (input view: user), to test different settings of our algorithm. We call this dataset Figurines3DSeg. Unlike quantitative results, computing 2D mask metrics for Acc and mIoU, we use metrics computed over actual Gaussians selected with our method againsts ground truth hand annotation.

Because our method tracks masks across viewes (§4), the choice of views is important. We compare using original scene training views against automatic dense views (§4.4.1) and the impact of the number of views  $m$  on quality and speed of our method in Tb3. We found  $m = 50$  to be optimal for performance as well as speed, completing full tracking (including Cutie inference) and 3D segmentation in only 1.5-2.5s. While this is not real-time, this delay is small enough to allow users to iterate with the algorithm in practice. For completeness, we also test with two different kinds of view

type of views (num.)	input view				Speed (s)	
	train		user			
	mIoU↑	Acc↑	mIoU↑	Acc↑		
training (all)	94.0	99.2	88.9	98.9	9-12s	
training (100)	93.9	99.2	93.3	99.1	3-4s	
training (50)	93.9	99.1	94.3	99.2	1.5-2.5s	
training (20)	92.8	99.0	94.0	99.2	0.6-1.2s	
training (10)	89.1	98.6	93.3	99.0	0.3-1s	
auto turnaround (100)	93.8	98.9	93.2	99.0	3-4.5s	
auto turnaround (50)	93.5	98.9	93.3	99.0	1.5-2.5s	
auto turnaround (20)	90.6	98.5	93.3	99.0	0.6-1.2s	
auto turnaround (10)	89.3	98.0	92.1	98.8	0.3-1s	
<b>no pre-segmentation</b>						
training (all)	83.88	98.4	76.9	97.8	26-27s	
auto turnaround (100)	89.0	98.2	90.7	98.6	8-9s	

Table 3. Segmentation Ablations on hand-labeled Figurines 3DGS scene.

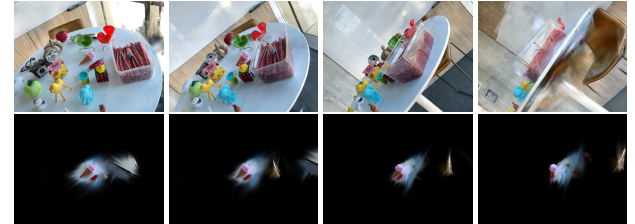


Fig. 6. Impact of presegmentation on the inputs to the tracker. Top: Input without presegmentation. Bottom: Input with presegmentation.

annotations, showing that our method generalizes to user-selected annotated views, making the interaction a lot less constrained. While we see some degradation when user-selected views are used, the usability still makes this feature attractive. In addition, we see a degradation in both speed and quality of the output when the pre-segmentation (§4.4.5 is turned off. This is because in the scenes with many objects, the tracked views may have occlusions. Pre-segmentation effectively removes some of the occluders in these views (See Fig.6).

## 6 Applications

Our selection and segmentation toolkit feeds into many downstream applications for 3DGS.

### 6.1 Interactive Orientation

Orienting a scene is important for consistent camera manipulation, and is critical for physics simulation, now possible directly on the 3DGS [Modi et al. 2024]. We observed that in most cases, the desirable XYZ axes coincide with the principal directions of variation for objects or surfaces. Our auto-orientation module allows users to automatically align the PCA basis computed over the means of the selected Gaussians with a chosen permutation of world axes. For example, the user could apply frustum projection to select a flat surface (Fig.9a1-3), then align Z axis with the axis of least variation (resulting in top capera view in Fig.9a 4) to achieve a consistent gravity direction. Manually orienting a scene is challenging, and we found this technique simple and effective when used in conjunction with our selection tools (§4).

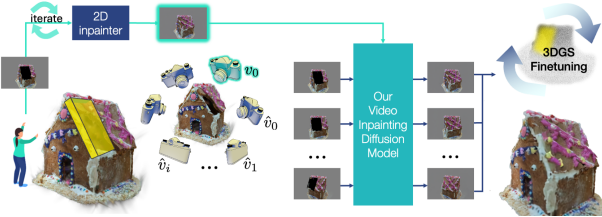


Fig. 7. **Object completion** (§6.2): after the user marks region to be completed and iterates on a 2D inpainting for one view, we apply a custom video inpainting model to propagate the result to multi-view consistent frames, which are used to fine-tune the 3DGS object.

## 6.2 User-Guided Editing

Unlike much of generative AI research, our objective is not to hallucinate large unseen areas. Instead, our method empowers future directions for targeted editing. This targeting is enabled through the various selection modes of our tool, providing different levels of precision. E.g. to indicate missing areas occluded parts during capture, the user can select the Gaussians around the hole using the paint tool. This selection could be used to generate masks for AI inpainting and be used to add new Gaussians. For editing existing areas, SAM selection can be used to efficiently remove parts. The paint tool can also be used to draw on interesting shapes to inpaint.

As a prototype towards targeted local editing, we experiment with a Video inpainting network that can be used to inpaint and optimize Gaussians only in the user-selected regions. We build our method on CogVideoX’s Image-to-Video model [Yang et al. 2024] as a strong video generation foundation and insert CamCo’s epipolar attention module [Xu et al. 2024] for camera control and 3D consistency. The inputs to our video model are masked video frames, binary masks for each frame, plucker embeddings and epipolar lines from camera parameters. The first frame of the video is a reference image that is generated by Stable Diffusion XL inpainting model. The typical user workflow would be to inpaint the first view using a text prompt, once satisfied, apply our video model to generate additional views starting from the first view. To propagate these changes to 3D, we remove the Gaussians that are selected and initialize new gaussians randomly inside the selection bounding box then train using the inpainted views. We show these early experiments to demonstrate how precise selection can help guide editing. Because we do not train on the unselected original Gaussians, we do not modify the look of the unselected area. We are excited to explore this application in future research.

## 6.3 Simulating Splat Objects

With the ability to segment, orient (§6.1) and refine (§6.2) it is becoming increasingly feasible to convert raw in-the-wild captures to simulated scenes. For example, 3DGS objects can be directly simulated using Simplicits [Modi et al. 2024] (See Fig.9b and video). Our flexible selection and segmentation toolkit also makes it possible for users to select individual object parts and assign different materials, for example to make the hair of the doll more deformable. This application is now directly possible using existing simulation techniques and our user-guided selection.

## 7 Conclusion

In conclusion, we presented ArtisanGS, a suite of versatile interactive selection and segmentation tools for 3D Gaussian Splats with AI and user in the loop. We believe that a flexible solution to user guided segmentation is a necessary foothold for many applications.

## References

Yongtang Bao, Chengjie Tang, Yuze Wang, and Haojie Li. 2025. Seg-Wild: Interactive Segmentation based on 3D Gaussian Splatting for Unconstrained Image Collections. In *Proceedings of the 33rd ACM International Conference on Multimedia* (Dublin, Ireland) (MM ’25). Association for Computing Machinery, New York, NY, USA, 8567–8576. <https://doi.org/10.1145/3746027.3755567>

Amir Barda, Matheus Gadelha, Vladimir G. Kim, Noam Aigerman, Amit H. Bermano, and Thibault Groueix. 2024. Instant3dit: Multiview Inpainting for Fast Editing of 3D Objects. arXiv:2412.00518 [cs.CV] <https://arxiv.org/abs/2412.00518>

Jiazhong Cen, Jiemin Fang, Chen Yang, Lingxi Xie, Xiaopeng Zhang, Wei Shen, and Qi Tian. 2023. Segment Any 3D Gaussians. *arXiv preprint arXiv:2312.00860* (2023).

Honghua Chen, Chen Change Loy, and Xingang Pan. 2024b. MVIP-NeRF: Multi-view 3D Inpainting on NeRF Scenes via Diffusion Prior. In *Proceedings of the IEEE/CVF Conference on Computer Vision and Pattern Recognition*, 5344–5353.

Yiwen Chen, Zilong Chen, Chi Zhang, Feng Wang, Xiaofeng Yang, Yikai Wang, Zhonggang Cai, Lei Yang, Huaping Liu, and Guosheng Lin. 2024a. Gaussianeditor: Swift and controllable 3d editing with gaussian splatting. In *Proceedings of the IEEE/CVF conference on computer vision and pattern recognition*, 21476–21485.

Ho Kei Cheng, Seoung Wug Oh, Brian Price, Joon-Young Lee, and Alexander Schwing. 2024. Putting the object back into video object segmentation. In *Proceedings of the IEEE/CVF Conference on Computer Vision and Pattern Recognition*, 3151–3161.

Ho Kei Cheng, Seoung Wug Oh, Brian Price, Alexander Schwing, and Joon-Young Lee. 2023. Tracking anything with decoupled video segmentation. In *Proceedings of the IEEE/CVF International Conference on Computer Vision*, 1316–1326.

Seokhun Choi, Hyeonseop Song, Jaechul Kim, Taehyeong Kim, and Hoseok Do. 2025. Click-gaussian: Interactive segmentation to any 3d gaussians. In *European Conference on Computer Vision*. Springer, 289–305.

Bin Dou, Tianyu Zhang, Yongjia Ma, Zhaohui Wang, and Zejian Yuan. 2024. Cosseg-gaussians: Compact and swift scene segmenting 3d gaussians. *arXiv preprint arXiv:2401.05925* (2024).

Kang Dou, Zhihao Liang, and Zeyu Wang. 2024. GS-ID: Illumination Decomposition on Gaussian Splatting via Diffusion Prior and Parametric Light Source Optimization. *arXiv preprint arXiv:2408.08524* (2024).

Sara Fridovich-Keil, Alex Yu, Matthew Tancik, Qinzhong Chen, Benjamin Recht, and Angjoo Kanazawa. 2022. Plenoxels: Radiance fields without neural networks. In *Proceedings of the IEEE/CVF conference on computer vision and pattern recognition*, 5501–5510.

Jian Gao, Chun Gu, Youtian Lin, Zhihao Li, Hao Zhu, Xun Cao, Li Zhang, and Yao Yao. 2025. Relightable 3d gaussians: Realistic point cloud relighting with brdf decomposition and ray tracing. In *European Conference on Computer Vision*. Springer, 73–89.

Qiao Gu, Zhaoyang Lv, Duncan Frost, Simon Green, Julian Straub, and Chris Sweeney. 2025. E golifter: Open-world 3d segmentation for egocentric perception. In *European Conference on Computer Vision*. Springer, 382–400.

Wenqi Hong, Ming Ding, Wendi Zheng, Xinghan Liu, and Jie Tang. 2022. CogVideo: Large-scale Pretraining for Text-to-Video Generation via Transformers. *arXiv preprint arXiv:2205.15868* (2022).

Xu Hu, Yuxi Wang, Lue Fan, Junsong Fan, Junran Peng, Zhen Lei, Qing Li, and Zhaoxiang Zhang. 2024a. SAGD: Boundary-Enhanced Segment Anything in 3D Gaussian via Gaussian Decomposition (or: Segment Anything in 3D Gaussians). arXiv:2401.17857 [cs.CV] <https://arxiv.org/abs/2401.17857>

Xu Hu, Yuxi Wang, Lue Fan, Junsong Fan, Junran Peng, Zhen Lei, Qing Li, and Zhaoxiang Zhang. 2024b. Semantic anything in 3d gaussians. *arXiv preprint arXiv:2401.17857* (2024).

Binbin Huang, Zehao Yu, Anpei Chen, Andreas Geiger, and Shenghua Gao. 2024. 2d gaussian splatting for geometrically accurate radiance fields. In *ACM SIGGRAPH 2024 Conference Papers*, 1–11.

Umangi Jain, Ashkan Mirzaei, and Igor Gilitschenski. 2024. GaussianCut: Interactive segmentation via graph cut for 3D Gaussian Splatting. *arXiv preprint arXiv:2411.07555* (2024).

Ying Jiang, Chang Yu, Tianyi Xie, Xuan Li, Yutao Feng, Huamin Wang, Minchen Li, Henry Lau, Feng Gao, Yin Yang, et al. 2024. Vr-gs: A physical dynamics-aware interactive gaussian splatting system in virtual reality. In *ACM SIGGRAPH 2024 Conference Papers*, 1–1.

Joji Joseph, Bharadwaj Amrutar, and Shalabh Bhatnagar. 2024. Gradient-Driven 3D Segmentation and Affordance Transfer in Gaussian Splatting Using 2D Masks. *arXiv preprint arXiv:2409.11681* (2024). <https://arxiv.org/abs/2409.11681>

Mihnea-Bogdan Jurca, Remco Royen, Ion Giosan, and Adrian Munteanu. 2024. RT-GS2: Real-Time Generalizable Semantic Segmentation for 3D Gaussian Representations of Radiance Fields. In *35th British Machine Vision Conference 2024, BMVC 2024, Glasgow, UK, November 25-28, 2024*. BMVA. <https://papers.bmvc2024.org/0299.pdf>

Bernhard Kerbl, Georgios Kopanas, Thomas Leimkühler, and George Drettakis. 2023. 3D Gaussian Splatting for Real-Time Radiance Field Rendering. *ACM Transactions on Graphics* 42, 4 (July 2023). <https://repo-sam.inria.fr/fungraph/3d-gaussian-splatting/>

Justin Kerr, Chung Min Kim, Ken Goldberg, Angjoo Kanazawa, and Matthew Tancik. 2023. LERF: Language Embedded Radiance Fields. In *International Conference on Computer Vision (ICCV)*.

Chung Min Kim, Mingxuan Wu, Justin Kerr, Ken Goldberg, Matthew Tancik, and Angjoo Kanazawa. 2024. Garfield: Group anything with radiance fields. In *Proceedings of the IEEE/CVF Conference on Computer Vision and Pattern Recognition*. 21530–21539.

Alexander Kirillov, Eric Mintun, Nikhila Ravi, Hanzi Mao, Chloe Rolland, Laura Gustafson, Tete Xiao, Spencer Whitehead, Alexander C Berg, Wan-Yen Lo, et al. 2023. Segment anything. In *Proceedings of the IEEE/CVF International Conference on Computer Vision*. 4015–4026.

Zhihao Liang, Qi Zhang, Ying Feng, Ying Shan, and Kui Jia. 2024. Gs-ir: 3d gaussian splatting for inverse rendering. In *Proceedings of the IEEE/CVF Conference on Computer Vision and Pattern Recognition*. 21644–21653.

Kunhao Liu, Fangneng Zhan, Muyu Xu, Christian Theobalt, Ling Shao, and Shijian Lu. 2024a. Stylegaussian: Instant 3d style transfer with gaussian splatting. In *SIGGRAPH Asia 2024 Technical Communications*. 1–4.

Kunhao Liu, Fangneng Zhan, Muyu Xu, Christian Theobalt, Ling Shao, and Shijian Lu. 2024b. StyleGaussian: Instant 3D Style Transfer with Gaussian Splatting. In *SIGGRAPH Asia 2024 Technical Communications (SA '24)*. Association for Computing Machinery, New York, NY, USA, Article 21, 4 pages. <https://doi.org/10.1145/3681758.3698002>

Yiren Lu, Jing Ma, and Yu Yin. 2024. View-consistent Object Removal in Radiance Fields. In *Proceedings of the 32nd ACM International Conference on Multimedia*. 3597–3606.

Ben Mildenhall, Pratul P. Srinivasan, Rodrigo Ortiz-Cayon, Nima Khademi Kalantari, Ravi Ramamoorthi, Ren Ng, and Abhishek Kar. 2019. Local Light Field Fusion: Practical View Synthesis with Prescriptive Sampling Guidelines. *ACM Transactions on Graphics (TOG)* (2019).

Ben Mildenhall, Pratul P. Srinivasan, Matthew Tancik, Jonathan T Barron, Ravi Ramamoorthi, and Ren Ng. 2021. Nerf: Representing scenes as neural radiance fields for view synthesis. *Commun. ACM* 65, 1 (2021), 99–106.

Vismay Modi, Nicholas Sharp, Or Perel, Shinjiro Sueda, and David IW Levin. 2024. Simplicits: Mesh-free, geometry-agnostic elastic simulation. *ACM Transactions on Graphics (TOG)* 43, 4 (2024), 1–11.

Nicolas Moenne-Loccoz, Ashkan Mirzaei, Or Perel, Riccardo de Lutio, Janick Martinez Esturo, Gavriel State, Sanja Fidler, Nicholas Sharp, and Zan Gojcic. 2024. 3D Gaussian Ray Tracing: Fast Tracing of Particle Scenes. *ACM Transactions on Graphics (TOG)* 43, 6 (2024), 1–19.

Thomas Müller, Alex Evans, Christoph Schied, and Alexander Keller. 2022. Instant Neural Graphics Primitives with a Multiresolution Hash Encoding. *ACM Trans. Graph.* 41, 4, Article 102 (July 2022), 15 pages. <https://doi.org/10.1145/3528223.3530127>

Francesco Palandra, Andrea Sanchietti, Daniele Baieri, and Emanuele Rodolà. 2024. GSEdit: Efficient Text-Guided Editing of 3D Objects via Gaussian Splatting. *arXiv preprint arXiv:2403.05154* (2024).

PlayCanvas. 2024. *SuperSplat*. <https://playcanvas.com/supersplat>

Zhongzheng Ren, Aseem Agarwala<sup>†</sup>, Bryan Russell<sup>†</sup>, Alexander G. Schwing<sup>†</sup>, and Oliver Wang<sup>†</sup>. 2022. Neural Volumetric Object Selection. In *IEEE/CVF Conference on Computer Vision and Pattern Recognition (CVPR)*. († alphabetic ordering).

Victor Rong, Jingxiang Chen, Sherwin Bahmani, Kiriakos N Kutulakos, and David B Lindell. 2024. GSTex: Per-Primitive Texturing of 2D Gaussian Splatting for Decoupled Appearance and Geometry Modeling. *arXiv preprint arXiv:2409.12954* (2024).

Quihong Shen, Xingyi Yang, and Xinchao Wang. 2025. Flashsplat: 2d to 3d gaussian splatting segmentation solved optimally. In *European Conference on Computer Vision*. Springer, 456–472.

Cyrus Vachha and Ayaan Haque. 2024. Instruct-GS2GS: Editing 3D Gaussian Splats with Instructions. <https://instruct-gs2gs.github.io/>

Zian Wang, Tianchang Shen, Merlin Nimier-David, Nicholas Sharp, Jun Gao, Alexander Keller, Sanja Fidler, Thomas Müller, and Zan Gojcic. 2023. Adaptive shells for efficient neural radiance field rendering. *arXiv preprint arXiv:2311.10091* (2023).

Ethan Weber, Aleksander Holynski, Varun Jampani, Saurabh Saxena, Noah Snavely, Abhishek Kar, and Angjoo Kanazawa. 2024. Nerfiller: Completing scenes via generative 3d inpainting. In *Proceedings of the IEEE/CVF Conference on Computer Vision and Pattern Recognition*. 20731–20741.

Jing Wu, Jia-Wang Bian, Xinghui Li, Guangrun Wang, Ian Reid, Philip Torr, and Victor Adrian Prisacariu. 2025. Gaussctrl: Multi-view consistent text-driven 3d gaussian splatting editing. In *European Conference on Computer Vision*. Springer, 55–71.

Tianyi Xie, Zeshun Zong, Yuxing Qiu, Xuan Li, Yutao Feng, Yin Yang, and Chenfanfu Jiang. 2023. PhysGaussian: Physics-Integrated 3D Gaussians for Generative Dynamics. *arXiv preprint arXiv:2311.12198* (2023).

Dejia Xu, Weili Nie, Chai Liu, Sifei Liu, Jan Kautz, Zhangyang Wang, and Arash Vahdat. 2024. CamCo: Camera-Controllable 3D-Consistent Image-to-Video Generation. *arXiv preprint arXiv:2406.02509* (2024).

Zhuoyi Yang, Jiayan Teng, Wendi Zheng, Ming Ding, Shiyu Huang, Jiazheng Xu, Yuanming Yang, Wenyi Hong, Xiaohan Zhang, Guanyu Feng, et al. 2024. CogVideoX: Text-to-Video Diffusion Models with An Expert Transformer. *arXiv preprint arXiv:2408.06072* (2024).

Mingqiao Ye, Martin Danelljan, Fisher Yu, and Lei Ke. 2025. Gaussian grouping: Segment and edit anything in 3d scenes. In *European Conference on Computer Vision*. Springer, 162–179.

Taoran Yi, Jiemin Fang, Junjie Wang, Guanjun Wu, Lingxi Xie, Xiaopeng Zhang, Wenyu Liu, Qi Tian, and Xinggang Wang. 2024. GaussianDreamer: Fast Generation from Text to 3D Gaussians by Bridging 2D and 3D Diffusion Models. In *CVPR*.

Haiyang Ying, Yixuan Yin, Jinzhi Zhang, Fan Wang, Tao Yu, Ruqi Huang, and Lu Fang. 2024. Omniseg3d: Omnipractical 3d segmentation via hierarchical contrastive learning. In *Proceedings of the IEEE/CVF Conference on Computer Vision and Pattern Recognition*. 20612–20622.

Haoyu Zhao, Hao Wang, Xingyue Zhao, Hongqiu Wang, Zhiyu Wu, Chengjiang Long, and Hua Zou. 2024. Automated 3D Physical Simulation of Open-world Scene with Gaussian Splatting. *arXiv preprint arXiv:2411.12789* (2024).

Yian Zhao, Wanshi Xu, Ruochong Zheng, Pengchong Qiao, Chang Liu, and Jie Chen. 2025. iSegMan: Interactive Segment-and-Manipulate 3D Gaussians. In *Proceedings of the Computer Vision and Pattern Recognition Conference (CVPR)*. 661–670.

Shijie Zhou, Haoran Chang, Sicheng Jiang, Zhiwen Fan, Zehao Zhu, Dejia Xu, Pradyumna Chari, Suya You, Zhangyang Wang, and Achuta Kadambi. 2024. Feature 3dgs: Supercharging 3d gaussian splatting to enable distilled feature fields. In *Proceedings of the IEEE/CVF Conference on Computer Vision and Pattern Recognition*. 21676–21685.

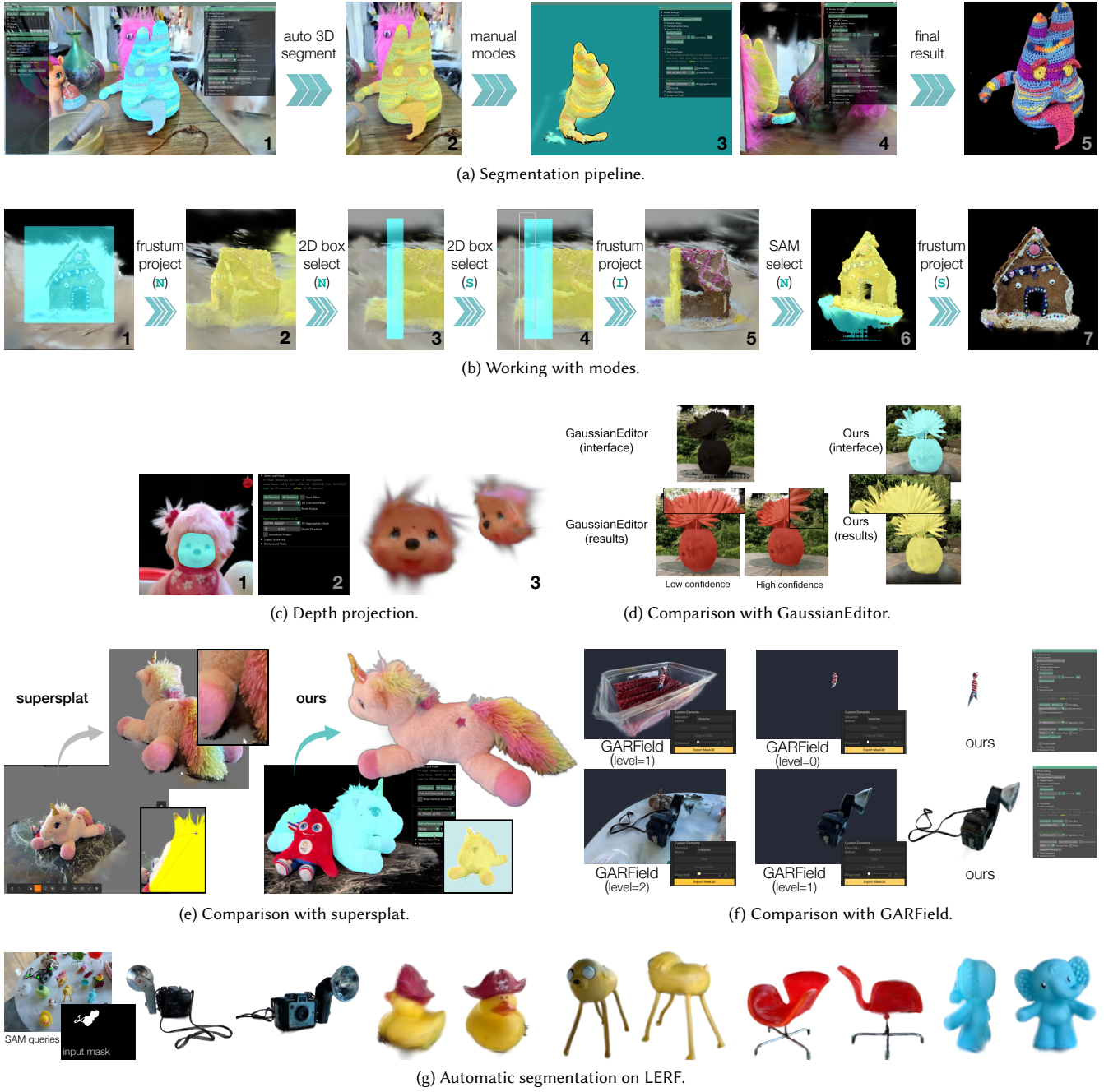
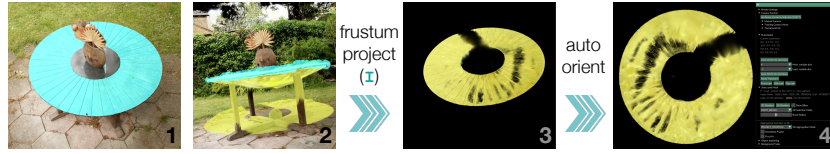


Fig. 8. **Segmentation Results:** We show the flexibility of our proposed segmentation toolkit (§4) in the figure above.

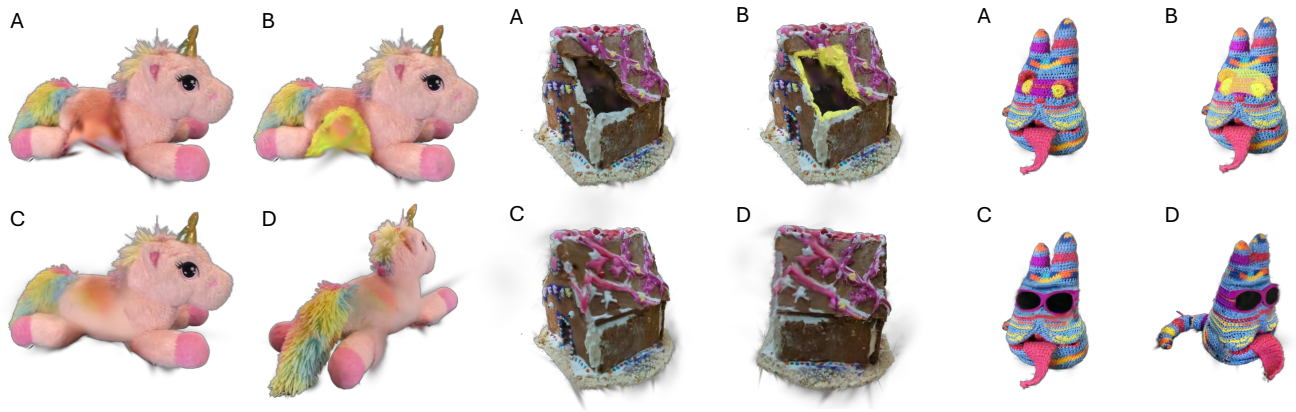
## Acknowledgments



(a) Orientation.



(b) Physics simulation of a 3DGS scene segmented with our method, using Simplicits [Modi et al. 2024].



(c) Targeted object editing with our method, showing original view (A), selected segment (B), and edited results (C, D).

Fig. 9. **Applications:** Our flexible segmentation toolkit can be used to enable user-guided orientation of 3DGS scenes (§6.1, Fig. 9a). Segmentation and orientation facilitate physics simulation directly over the captured 3DGS scene (§6.3, Fig. 9b). Controllable selection also enables targeted object editing (§6.2, Fig. 9c).

## A Comparison to Standard Software

Under controlled object-centric conditions (even as simple as suspending an object on a string), it is possible to capture data where one can easily select objects using simple techniques like bounding boxes. However, there are many scenarios ‘in the wild’ where this might not be possible. Editing tasks, like moving or removing specific objects, are heavily dependent on good selection tools. A number of standard software applications address this problem: Gaussian splat capturing solutions like Scaniverse [Niantic 2024] or Polycam [Polycam 2024] allow bounding volume based selection. In addition KIRI Engine [KIRI Innovations 2024] as well as Postshot [Jawset 2024] feature brush based selection, in many cases the focus here is object extraction via deletion of unwanted parts of the scan. Gaussian Splatting [Irrealix 2024a,b] for After Effects [Adobe Systems 2024] and Nuke [Foundry 2024] allow integration of Gaussian Splatting into 2.5d image compositing pipelines - their feature set matches the above. Dedicated Gaussian splat web apps like Supersplat [PlayCanvas 2024] as well as extensions to game engines XVERSE 3D-GS UE Plugin [XVERSE Technology Inc. 2024] for Unreal Engine [Epic Games 2024b] or SplatVFX [Keijiro 2023] for Unity [Unity Technologies 2024] expand the editing capabilities by allowing manipulation using their standard tooling on a point level. Extensions to standard 3D animation software like NerfStudio [nerfstudio 2024] for Blender [The Blender Foundation 2024] offer a similar feature set. In addition to cleanup, segmentation is used here often to extract or modify individual features from a scan for downstream use. GSOPs [Rhodes and Diaz 2024] for Houdini [SideFX 2025] not only opens up the the use Houdini’s direct and procedural tools for direct and indirect feature selection for Gaussian Splat models, but also adds automatic clustering and segmentation based on the DBSCAN algorithm [Ester et al. 1996].

While user-guided feature selection in Gaussian Splatting data is the main focus of this paper, we nevertheless consider feature selection in point cloud or volumetric data for industrial or medical uses closely related: ReCap Pro [Autodesk 2024], Reality Capture [Epic Games 2024a] and PIX4Dmatic [Pix4D 2024] are photogrammetry solutions used in surveying, where a user might need to identify elements of a scan (for example part of a worksite) for further inspection.

In addition to the standard selection tools found in 3D-animation software, we can find automatic and semi-automatic solutions that help dealing with often large data volumes: Segments AI [Segments.ai 2024], Pointly [Pointly GmbH 2024], Metashape [Agisoft LLC 2024] and ArcGIS [Esri 2024] offer automatic machine learning based feature classification for large scale data-labeling needs with application in fields like city mapping or autonomous driving. In medical imaging, a radiologist might need to select a organ from a volumetric CT scan for further analysis. 3D Slicer [Various 2024] is a popular tool that allows to automatically select such features from a volumetric scan using machine learning with extensions like TotalSegmentator [Wasserthal et al. 2023]. Here, ‘region growing’ is a semi-automatic technique where a user identifies ‘seed points’ in features used as reference data points for similarity based selection expansion.

	Ours		Ours (without pre-segmentation)	
	mIoU	Acc	mIoU	Acc
fern	83.6	94.7	83.6	94.8
flower	97.9	99.5	97.9	99.5
fortress	98.5	99.7	98.3	99.7
horns left	0.0	94.0	92.7	99.4
horns center	97.4	99.4	97.4	99.4
leaves	96.4	99.8	96.6	99.8
orchids	96.6	99.2	96.7	99.2
trex	89.2	98.5	89.2	98.6

Table 4. NVOS Segmentation evaluation. The “horns\_left” is failing with pre-segmentation because the object is partially out of frame in the input mask.

With Gaussian Splatting being adopted for industry use-cases, we believe our research to be applicable and complementary to existing tooling in these domains, too.

## B Evaluation Details

Breakdown of the NVOS results per testcases is presented in Table 1, showing that pre-segmentation only affects one example.

## References

Pointly GmbH. 2024. *Pointly*. <https://pointly.ai>  
 Adobe Systems. 2024. *After Effects*.  
 Agisoft LLC. 2024. *Agisoft Metashape*. <https://www.agisoft.com>  
 Autodesk. 2024. *ReCap Pro*. <https://www.autodesk.com/products/recap>  
 Epic Games. 2024a. *RealityCapture*. <https://www.capturingreality.com>  
 Epic Games. 2024b. *Unreal Engine*. <https://www.unrealengine.com>  
 Esri. 2024. *ArcGIS*. <https://www.arcgis.com>  
 Martin Ester, Hans-Peter Kriegel, Jörg Sander, and Xiaowei Xu. 1996. A Density-Based Algorithm for Discovering Clusters in Large Spatial Databases with Noise. *Proceedings of the Second International Conference on Knowledge Discovery and Data Mining (KDD-96)* (1996), 226–231.  
 Foundry. 2024. *Nuke*. <https://www.foundry.com/products/nuke-family/nuke>  
 Irrealix. 2024a. *Gaussian Splatting for After Effects*. <https://aescritps.com/gaussian-splatting/>  
 Irrealix. 2024b. *Gaussian Splatting for Nuke*. <https://aescritps.com/gaussian-splatting-for-nuke>  
 Jawset. 2024. *Postshot*. <https://www.jawset.com>  
 Takahashi Keijiro. 2023. *SplatVFX*. <https://github.com/keijiro/SplatVFX>  
 KIRI Innovations. 2024. *KIRI Engine*. <https://kiriengine.app>  
 nerfstudio. 2024. *Nerfstudio Blender Add-on*. [https://docs.nerf.studio/extensions/blender\\_addon.html](https://docs.nerf.studio/extensions/blender_addon.html)  
 Niantic. 2024. *Scaniverse*. <https://scaniverse.com>  
 Pix4D. 2024. *PIX4Dmatic*. <https://www.pix4d.com>  
 PlayCanvas. 2024. *SuperSplat*. <https://playcanvas.com/supersplat>  
 Polycam. 2024. *Polycam*. <https://polycam/>  
 David Rhodes and Ruben Diaz. 2024. *GSOPS: Gaussian Splatting Operators for Houdini*. <https://github.com/david-rhodes/GSOPS>  
 Segments.ai. 2024. *Segments.ai*. <https://segments.ai>  
 SideFX. 2025. *Houdini*. <https://www.sidefx.com/products/houdini/>  
 The Blender Foundation. 2024. *Blender*. <https://www.blender.org/>  
 Unity Technologies. 2024. *Unity*. <https://unity.com>  
 Various. 2024. *3D Slicer*. <https://slicer.org>  
 Jakob Wasserthal, Michael Meyer, Hanns-Christian Breit, Joshy Cyriac, Yanyi Shan, and Michael Segeroth. 2023. TotalSegmentator: robust segmentation of 104 anatomical structures in CT images. *arXiv preprint arXiv:2208.05868* (2023). <https://github.com/lassoan/TotalSegmentator> Version 2.  
 XVERSE Technology Inc. 2024. *XVERSE 3D-GS UE Plugin*. <https://github.com/XVERSE-Engine/XV3DGS-UEPlugin>